

# Homology model and potential virus-capsid binding site of a putative HEV receptor Grp78

Hai Yu · Shaowei Li · Chunyan Yang · Minxi Wei ·  
Cuiling Song · Zizheng Zheng · Ying Gu · Hailian Du ·  
Jun Zhang · Ningshao Xia

Received: 20 April 2010 / Accepted: 25 June 2010 / Published online: 14 July 2010  
© Springer-Verlag 2010

**Abstract** P239, a truncated construct of the hepatitis E virus (HEV) ORF2 protein, has been proven able to bind with a chaperone, Grp78, in both an in vitro co-immune precipitation test and an in vivo cell model. We previously solved the crystal structure of E2s—the C-terminal domain of p239 involved in host interactions. In the present study, we built a 3D structure of Grp78 using homology modeling methods, and docked this molecule with E2s using the Zdockpro module of the InsightII software package. The modeled Grp78 structure was deemed feasible by profile 3D evaluation and molecular dynamic simulations. The docking result consists of six clusters of distinct complexes and C035 was selected as the most reasonable. The interacting interface of the predicted complex is comprised of the Grp78 linker region and nucleotide binding domain along with the E2s groove region and surrounding loops. Using energy, hydrogen bond and solvent accessible surface analyses, we identified a series of key residues that may be involved in the Grp78:E2s interaction. By comparing with the known structure of the Hsp70:J complex, we further concluded that the interaction of Grp78 and E2s could interrupt binding of Grp78 with the J domain, and in turn diminish or even eliminate the binding ability of the Grp78 substrate binding domain. The predicted series of key residues also provides clues for further research that should improve our understanding of the fundamental molecular mechanisms of HEV infection.

**Keywords** Grp78 · Hepatitis E virus · Homology modeling · Molecular docking

## Introduction

Hepatitis E virus (HEV) is an important cause of severe acute hepatitis and accounts for high mortality in pregnant women who develop fulminant liver disease [1]. The HEV genome is a positive-stranded RNA of approximately 7.5 kb that includes three open reading frames (ORF1–3). ORF2 encodes a single structural protein of 660 amino acids (aa). The protein form dimers, which constitute the viral capsomeres, which in turn are subunits of the viral capsid [2]. Our previous studies on a truncated recombinant of the ORF2 protein (aa368–aa606, p239 protein) suggested that this fragment can form 23 nm-diameter particles and subsequently penetrate susceptible cells in a manner similar to that of wildtype virus. We also reported for the first time the 2.0 Å-resolution crystal structure of E2s (aa455–aa602) (pdb ID 3ggq). This structure exhibits a  $\beta$ -barrel architecture consisting of an internal hydrophobic pore, with both sides of the  $\beta$ -barrel blocked by short loops. Further experiments showed that this domain lies in the protruding region of the HEV capsid that is likely to be involved in host interactions for effective propagation of viral infection [3].

Our earlier studies showed that the ORF2 fragment p239 (aa368–aa606) can bind a chaperone known as Grp78 both in vitro and in vivo [4, 5]. Grp78 is a member of the 70-kDa heat shock protein (HSP70) family that is involved in many cellular processes, including regulation of calcium homeostasis, translocation of newly synthesized polypeptides across the endoplasmic reticulum membrane, and their subsequent folding, maturation, transport or retrotranslocation. Hsp70

H. Yu · S. Li (✉) · C. Yang · M. Wei · C. Song · Z. Zheng ·  
Y. Gu · H. Du · J. Zhang · N. Xia  
National Institute of Diagnostics and Vaccine  
Development in Infectious Diseases, School of Life Science,  
Xiamen University,  
Xiamen, Fujian Province, China  
e-mail: shaowei@xmu.edu.cn

proteins consist mainly of two domains: a 44-kDa N-terminal domain and a 30-kDa C-terminal domain. The former carries a weak ATPase activity (nucleotide binding domain, NBD) [6, 7], and the latter can be further divided into two parts: a 20-kDa  $\beta$ -sandwich domain and a 10-kDa C-terminal  $\alpha$ -helical subdomain [8, 9]. The  $\beta$ -sandwich domain contains a substrate binding site (substrate binding domain, SBD) with which it can bind various hydrophobic peptides and regulate their post-translational processing. A short linker of about 13 residues connects the NBD and the SBD. As a resident of endoplasmic reticulum (ER) chaperone, the expression of Grp78 is upregulated in response to ER stress in mammalian cells [10]. Although the effect of Grp78 induction on virus replication is not fully understood, accumulating evidence suggests that various viral proteins trigger its expression during virus infection. These viruses include simian virus 5 [11], respiratory syncytial virus [12], flaviviruses and hantavirus [13, 14]. On the other hand, Grp78 can bind to viral proteins and perform at least two distinct functions, including facilitating the folding or assembly of viral proteins, and detecting and disaggregating the unfolded or misfolded viral proteins [15, 16]. We have previously found that Grp78 can bind to the HEV capsid protein [4] and proposed that Grp78 may be involved in endocytosis of HEV as it can be detected on both membrane and ER. Considering the natural function of Grp78, this binding also suggests that this chaperone may play a role in the viral life cycle. In this study, we build a structure of Grp78 using the homology modeling method, and dock this molecule with our newly published E2s structure. Upon analysis of the most likely complex, we concluded that a series of key residues may be involved in the interaction. The complex structure of Hsp70 and the J domain of J chaperone has been reported by Jiang [17], and the binding of Grp78 and another J chaperone homolog MTJ1 has also been proved [18]. Comparing these structures with our predicted structure, we also propose that the interaction of Grp78 and E2s may interrupt Grp78–J binding and then deactivate Grp78 ATPase and subsequent substrate binding. Further research on interactions between viral capsid proteins and chaperone proteins should improve the understanding of the fundamental molecular mechanisms of HEV infection.

## Methods

### Homology modeling of Grp78

The sequence of human Grp78 was obtained from GenBank (accession number AF216292). Using the Protein Data Bank BLAST search, eight crystal structures, all belonging to the same family of 70kD heat shock proteins, including Grp78 (PDB no. 1yuw:68%, 3hsc:69.9%,

2v7z:69.4%, 2qw9:69.9%, 1hpm:70%, 2e88:67.3%, 1dg4:61.3%, 1dkx:46.6%, reported from different laboratories and different methods were selected as homology modeling templates [7, 8, 17, 19–22]. Average identities between the target sequence (Grp78) and templates are relatively high (up to 67%). The initial 3D model of the Grp78 structure was generated using the Homology module of the InsightII 2005 software packages on an IBM IntelliStation Z Pro workstation. In the subsequent minimization and dynamics simulation, stepwise minimization was used to ensure the correct relaxation of our initial model. Using CHARMM force field [23], the 200-steps steepest-descent method and 1,000-steps conjugate gradient method with different constraints, including fixed structurally conserved regions (SCR), fixed heavy atoms, fixed main chains and fixed  $\alpha$ -carbon, respectively, minimization was carried out on the InsightII CHARMM module. The final structure of Grp78 was evaluated using Profile 3D [24], PROCHECK (PDBsum tools on <http://www.ebi.ac.uk/pdbsum/>) and Ramachandran plot assay. The model was embedded with a 7 Å water layer and minimized with the whole Grp78 model fixed. The fixed constraint was then removed and a 500 ps dynamics simulation was performed at 298 K and constant volume to examine the stability of the model.

### Preparation of E2s structure

The structure of E2s had been determined in our previous study: PDB ID 3ggq. Before being submitted to the docking program, the E2s structure was also embedded explicitly with a 7 Å water layer and optimized using a standard dynamic cascade, which includes two steps of minimization (steepest 500 steps and conjugate 2,000 steps), and 50 ps heating, 100 ps equilibration and 500 ps NVT production simulations.

### Molecular docking of Grp78 and E2s

The E2s and optimized Grp78 structures were submitted to the ZDockpro module of the InsightII 2005 package with the former taken as ligand and the latter as receptor. The general protocol for running ZDockpro includes two consecutive steps of calculation described as geometry search and energy search [25, 26], running in program ZDock and RDock respectively. The first 1,000 poses in ZDock result were chosen for RDock calculation. The filter in the resultant docking poses was set in light of the functional implications of these molecules except for the theoretic restriction in silico as mentioned in our previous study [27]. From the RDock result, poses with both high ZRank and RRank (Scores in ZDock and RDock) were selected as candidates for further analysis. To screen for the

most reasonable docking result, all candidates were superimposed into a VLP surface of ORF2 (PDB number: 3hag) by alignment of the E2s region. Complexes having Grp78 bumping with the surface of VLP were excluded.

### Optimization and analysis of the complex structures

The final complex structures were submitted to minimization and dynamics simulation as described above and the lowest-energy conformation was selected from the energy trajectory. The total energy and the interaction energy were then calculated. Further analysis of the complexes included hydrogen bond analysis and solvent accessible surface (SAS) analysis.

## Results and discussion

### Homology modeling of Grp78 and model evaluation

Grp78 is a member of the Hsp70 chaperone family. Research on this family of proteins has been ongoing for nearly two decades, resulting in definite structures for many of the homologues in the same family. In our homology project, the templates for modeling Grp78 belong to a common family, and the average identity in sequences between Grp78 and the templates reaches 67%. Although we found eight known crystal or NMR structures, all with a high similarity in sequence to Grp78, most of the templates contain only one of the two domains, except 1yuw. The alignment of these templates against the target Grp78 sequence is shown in Fig. 1 in two parts to address the regions of the matched structures. These matched structures were taken as the structures of the corresponding regions in the target sequence. The final optimized modeled structure of Grp78 resembles the structure of 1yuw (RMSD  $\approx$  0.65 Å), which contains an N-terminal domain and a C-terminal domain connected by a linker region (Fig. 2a). Figure 2b shows the structure colored according to structurally conserved regions (SCRs). It can be clearly observed that most of the SCRs are located within SBD, and NBD has only short, scattered SCRs. Although the C-terminal region presents low sequence similarity compared with the templates, the optimized modeled structure also exhibits an intact, four-stranded, anti-parallel  $\beta$ -sheet sandwich as previously described by NMR [28]. After the molecular dynamics (MD) simulation described above, the structures of Grp78 NBD and SBD were individually superimposed onto the 1yuw structure (Fig. 2e, f). NBD exhibits better superimposition in the IA and IIA (RMSD 2.897) lobes than in the IB and IIB lobes (RMSD 4.588), suggesting that the latter exhibits more flexibility in the molecular dynamics simulation. At the C-terminal domain,

despite low sequence similarity, the SBD still shares topology with the template. Ramachandran plot and PROCHECK results from the initial Grp78 model showed that only seven amino acid (1.3%, glycine excluded) are in the disallowed area, and all of them are located near the C-terminal of SBD, indicating that our initial model can be safely used in the following MD simulation and docking analysis. In Profile-3D evaluation, the sum of the self-compatibility score for the model is 238.83, which is between the low and high scores expected for the corresponding structure (126–280). From the plot of local compatibility scores (Fig. 3), nearly all of the residues show correct folding except the ravine in the region around residue 450, which also appears in the plot of 1yuw. A plot of the potential energy versus time of the MD simulation is displayed in Fig. 2b. The potential energy decreases substantially in the first 100 ps of the dynamics simulation and stabilized at about  $-8,600$  kcalmol $^{-1}$ . The RMSD value remains at  $\sim 4.0$  Å after equilibration (Fig. 2c). Just before this work was submitted, an NBD structure of Grp78 (aa28–406, full length 654aa) was published in the Protein Data Bank (3iuc) [29]. However, this structure is a single domain of Grp78 with a folding similar to that of part of other homologous protein (HSP70, and others). Functionally, docking with E2s for mapping interaction interface of Grp78 entails a structural model of the full-length Grp78. In the present study, superimposed with 3iuc structure, the final Grp78 model exhibit a lower RMSD of 1.083 Å, which indicates it is a highly accurate homology model (Fig. 2d) [30]. All of this evidence indicates that the modeled Grp78 is reasonable not only in terms of stereochemistry but also in energy stability, and that it can be used for subsequent docking calculation.

### Docking of Grp78 and E2s

We have previously shown that the E2s domain is the shortest fragment of HEV ORF2 needed for dimerization and neutralization function [3, 31, 32]; the E2s domain is located in the protruding part of the virus shell [33, 34]. Structurally, it could serve as a putative receptor binding site being on the outmost part of virus shell [3, 35]. Functionally, Grp78 acts as a host receptor and the E2s dimer as the ligand. Docking calculations take a snapshot of the binding moment. By examining the top 100 poses of the sorted RDock result, many complex structures were found to be analogues. Six different structures that ranked highly and occurred the most often were selected for further screening. The six different complexes (C035, C277, C290, C441, C779, C859—the number represent the rank score in ZDock calculation) represent six clusters of poses in the first 100 RDock results. When superimposing with the HEV VLP structure by alignment of E2s, four structures

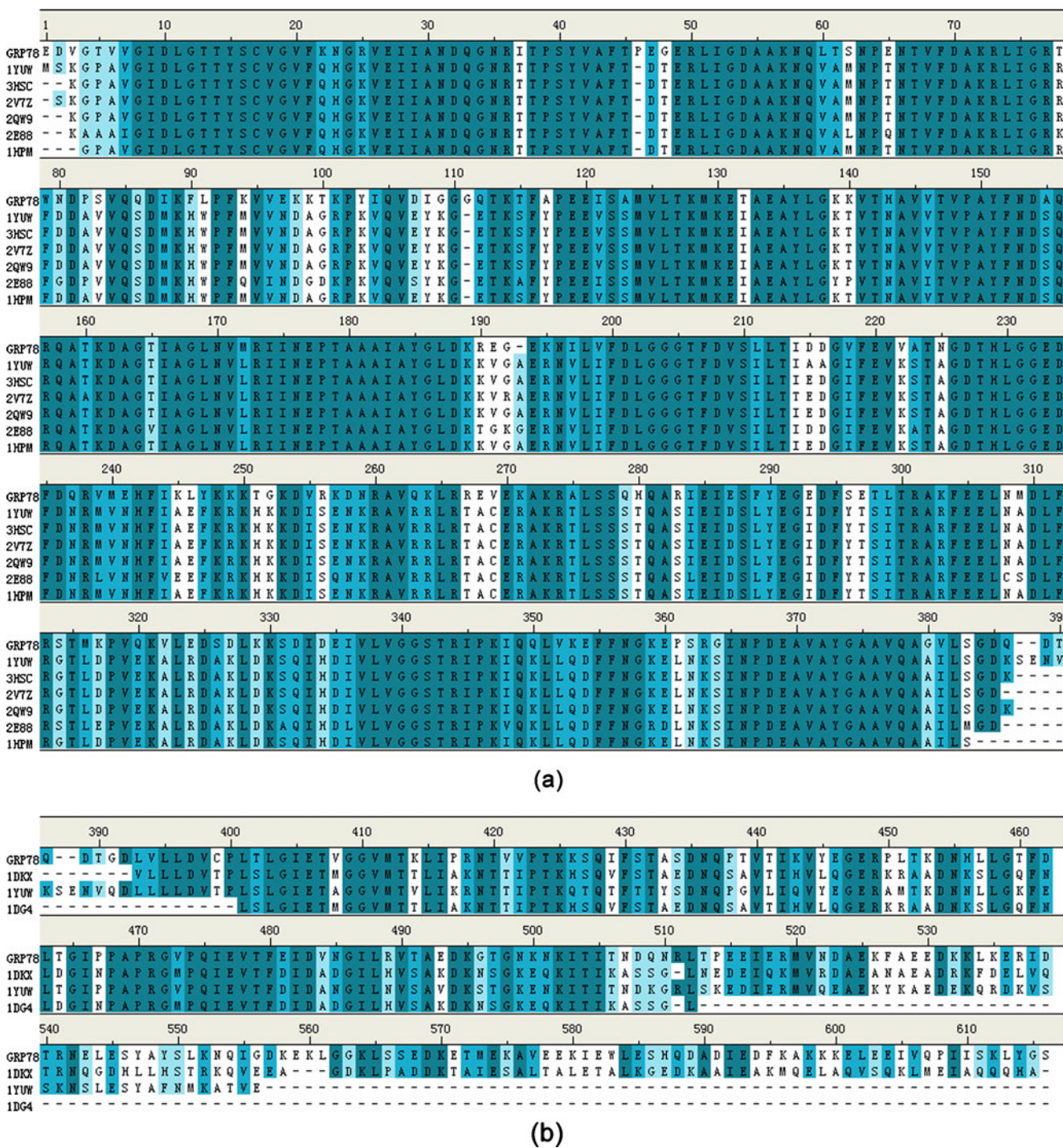
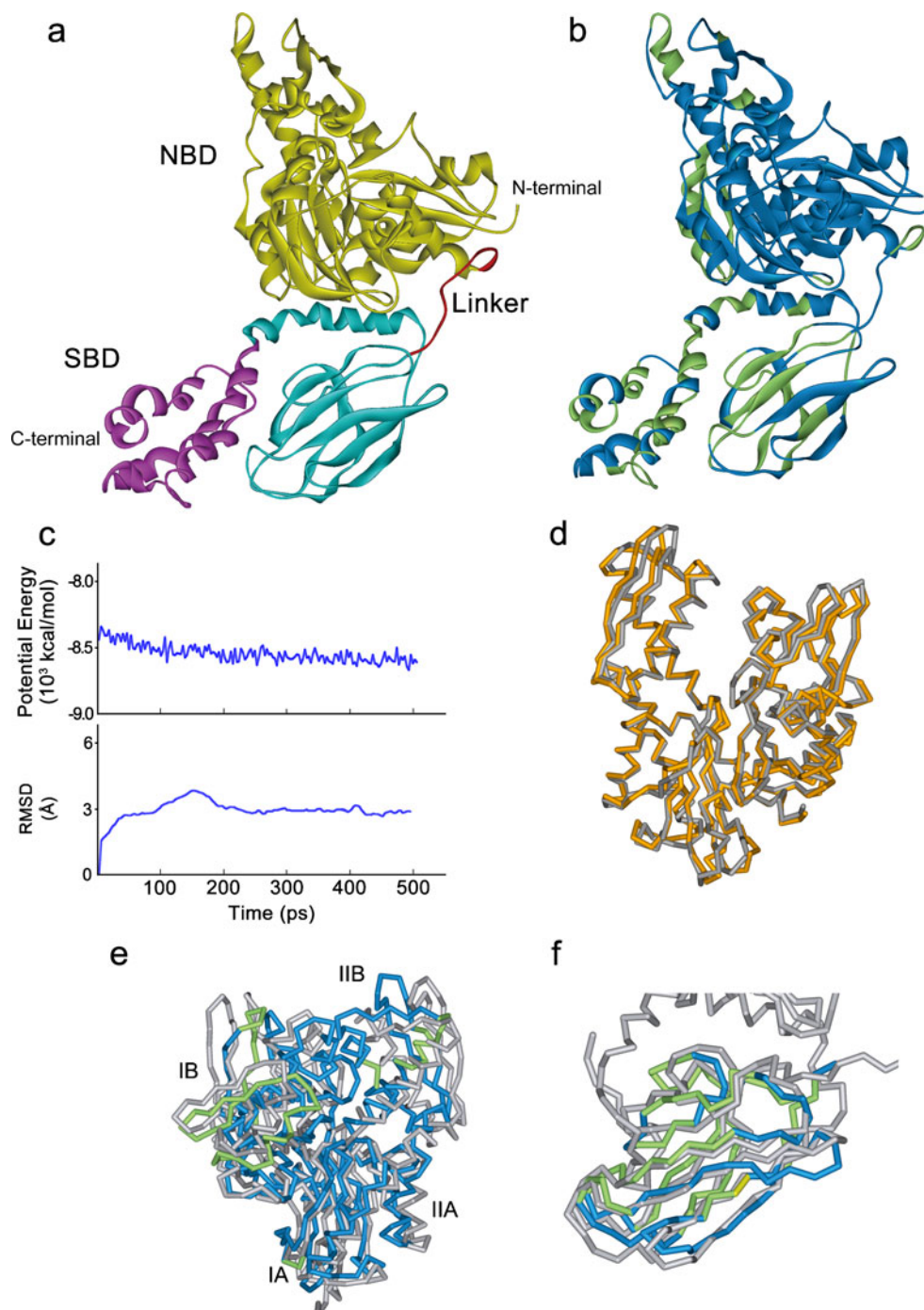


**Fig. 1** Multiple sequence alignment of Grp78 with templates sequences. **a** Alignment of aa1–386, **b** alignment of aa385–end

(C277, C290, C441 and C779) were excluded due to detection of bumping between Grp78 and the surface of VLP surrounding the E2s region. The remaining complexes, C035 and C859, have their interaction interfaces located near the groove region of E2s. Generally, a structure having high scores in both ZDock and RDock may be considered a candidate structure for interaction. In the

present study, C035 was selected as the most reasonable structure (Fig. 4). In the structure of complex C035, one of the monomers in the E2s dimer has its groove region facing the kinked alpha helix ( $\alpha$ A) of the SBD and a 6 $\beta$ -strand contacting the 5 $\beta$ -strand of the SBD. The other monomer connects the Grp78 linker with its coiled loop only between the 10 $\beta$ - and 11 $\beta$ - strands. Interestingly, we had previously

**Fig. 2** 3D structure of the homology-modeled Grp78. **a, b** The structure is displayed as a *solid ribbon diagram*. **a** *Yellow* nucleotide binding domain (NBD), *red* linker region, *cyan* substrate binding domain (SBD), *magenta* C-terminal helix region. **b** *Blue* structurally conserved regions (SCRs), *green* other regions. **c** Potential energy and root mean square deviation (RMSD) with respect to simulation time for 500 ps molecular dynamics simulation on Grp78 model. **d** NBD of homology model (*orange*) superimposed on published structure 3iuc (*gray*). **e, f** NBD and SBD superimposed on template 1yuw (*silver*), respectively



identified the groove region as being associated with the interaction between E2s and neutralizing antibodies by alanine scanning mutagenesis [3].

**Key residues involved in interaction between Grp78 and E2s**

The ultimate docking hit of the complex model was submitted to a 500 ps MD simulation, which resulted in a more stable conformation in terms of an equilibrium state during

simulation. The total energy of C035 is  $-7,796.77$  kcal mol<sup>-1</sup>, lower than the sum of individual E2s and Grp78 ( $-7,481.57$  kcal mol<sup>-1</sup>). Interaction energy was calculated using CHARMM in the simulation module of the Discovery Studio. The interaction energy is defined as the sum of the van der Waals and electrostatic energy and the value is broken down per-residue for each residue located at the interface. Most of the residues with high interaction energy are involved in the short strong hydrogen bond between the ligand and receptor (Table 1). The key residues involved in

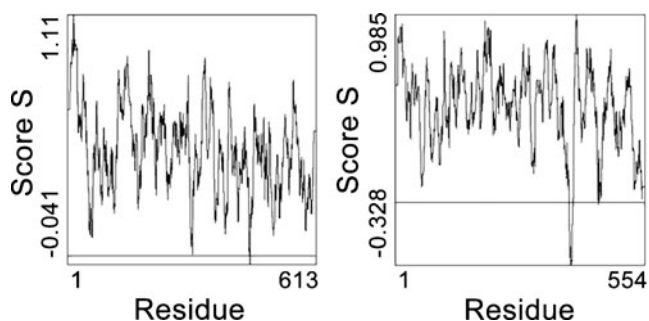


**Fig. 3** 3D profiles test of the final protein model of Grp78 (*left*) and the template protein model 1yuw (*right*)

the interaction were screened for using the following parameters: (1) Hydrogen bond analysis. Hydrogen bond analysis was combined with a 200 ps dynamics simulation at 298 K. Atomic coordinates were saved every 1 ps and hydrogen bond formation was monitored for each conformation to find the most stable. Hydrogen bonds occurring with a frequency higher than 90% were considered as stable and enrolled with average distances in Table 2. Distances less than 2.7 Å were considered as short strong hydrogen bonds (SSHB), and these residues were in accord with the above mentioned interaction energy analysis. All these SSHB-driven interactions would stabilize the binding of Grp78 and E2s. In addition, we also detected triadic hydrogen bonds (Thr527:Arg524:Asn528, Asn194:Tyr561:Val195), which may strengthen the H-bond strength and sometimes shows the catalytic effect in certain biosystems [36–38]. The distances between these H-bonds are all less than 2.7 Å, and we can safely predict that these residues play a very important role in the interaction. (2) SAS analysis.

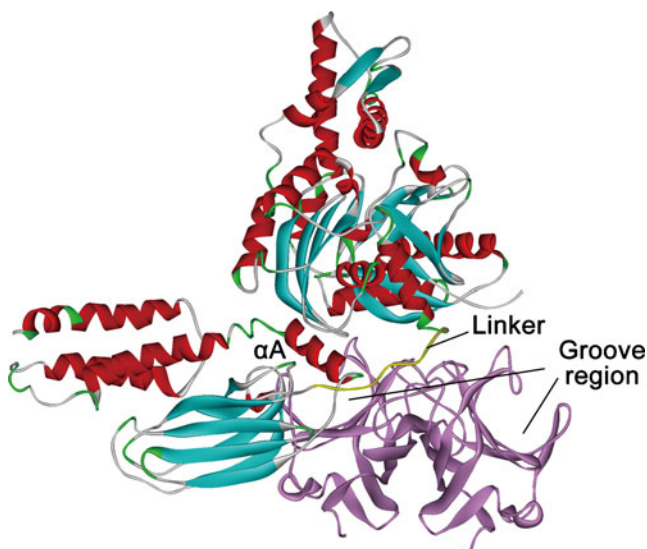


**Fig. 4** Structure of complex C035. Grp78 and E2s are displayed as a solid ribbon diagram. Grp78 is colored by secondary structure type. Purple E2s, yellow linker region of Grp78

**Table 1** Statistics of interaction energy of each residue located at the interface of the C035 structure. Calculation is based on the force field CHARMM. Values are in kcal mol<sup>-1</sup>

Residue <sup>a</sup>	Interaction energy	van der Waals interaction energy	Electrostatic interaction energy
Total	-310.18	-144.76	-165.42
E2S_1_ARG524 <sup>b</sup>	-34.171299	-4.75968	-29.4116
GRP78_GLU536	-28.494499	-2.39298	-26.1015
GRP78_ASP410	-22.8762	-7.23293	-15.6433
E2S_2_LYS554	-19.888	-2.35093	-17.5371
GRP78_ASP475	-19.2591	-6.08354	-13.1756
E2S_1_GLN530	-17.997601	-7.66603	-10.3316
GRP78_LEU405	-17.9779	-8.48628	-9.4916
E2S_1_THR528	-17.163601	-6.77512	-10.3885
E2S_1_TYR584	-15.8513	-5.97149	-9.87984
E2S_1_THR563	-15.723	-4.33566	-11.3873
GRP78_VAL195	-15.6353	-2.24305	-13.3922
GRP78_ASP178	-15.5447	-6.62641	-8.91833
E2S_1_TYR561	-14.285	-3.63752	-10.6475
GRP78_ASP544	-13.0622	-1.03119	-12.031
E2S_1_SER527	-12.6511	-3.77438	-8.87671
GRP78_LEU478	-12.0741	-5.73856	-6.33553
E2S_1_ASN560	-11.9751	-2.8743	-9.10077
E2S_1_GLN531	-11.6716	-2.78592	-8.88564
E2S_1_THR489	-11.6295	-5.9444	-5.68514
E2S_2_TYR584	-11.3738	-5.38477	-5.98905
GRP78_ASN476	-11.0835	-2.22147	-8.86208
GRP78_ASN194	-10.8448	-3.42011	-7.42466
E2S_2_TYR561	-10.7184	-5.37708	-5.3413
GRP78_SER406	-10.0699	-4.51537	-5.55451

<sup>a</sup> Only interaction energies higher than 10 kcal mol<sup>-1</sup> are shown

<sup>b</sup> E2s\_1 and E2s\_2 represent each monomer of the E2s dimer

**Table 2** Statistics of the occurrence (Freq.) of hydrogen bond (>90%) during a 200 ps dynamic simulation of the C035 structure

Hydrogen bond	Freq. (%)	Distance (Å)
E2s:Asn562:ND2–GRP78:Met196:SD	100	2.32
E2s:Arg524:NH1–GRP78:Asn528:OD1	100	2.37
E2s:Tyr561:OH–GRP78:Asn194:ND2	100	2.64
E2s:Tyr561:OH–GRP78:Val195:O	99	2.69
E2s:Arg524:NH1–GRP78:Thr527:O	98	2.13
E2s:Thr489:OG1–GRP78:Asp178:OD1	97	3.29
E2s: Tyr584:OH–GRP78:Val195:O	96	2.33
E2s:Thr586:OG1–GRP78:Asp410:O	95	3.11
E2s: Thr489:OG1–GRP78:Asp178:OD2	91	2.94

**Table 3** Changes in solvent accessible surface (SAS) areas

Res <sup>a</sup>	Index <sup>b</sup>	cSAS <sup>c</sup>	iSAS <sup>d</sup>	$\Delta$ SAS(>40%)
Ser	C406	1.6	53.8	52.2
Gln	C409	45.3	90.6	45.3
Gln	C530	10.5	54.7	44.2
Pro	C535	8.8	55.4	46.6
Glu	C536	8.7	55.3	46.6
Ser	A488	12.5	67.1	54.6
Arg	A524	20.5	65	44.5
Pro	A525	36.2	77.8	41.6
Ser	A527	4.2	56.6	52.4
Gln	A530	24.7	69.6	44.9
Ala	A565	0.8	50.9	50.1
Gly	B589	0.3	40.7	40.4

<sup>a</sup> Residues with a  $\Delta$ SAS value higher than 40% are listed

<sup>b</sup> C represents Grp78, A/B represents the two monomers of E2s

<sup>c</sup> SAS values (%) of the C035 structure

<sup>d</sup> SAS values (%) of the residue in individual proteins (Grp78 or E2s)

Relative SAS areas (%) of each residue in the complex structure and individual proteins were calculated, and  $\Delta$ SAS values are listed in Table 3. In the Insight II package, the tripeptide model was used to normalize the surface area, which eliminates effects due to different residue types. Residues with higher  $\Delta$ SAS were considered to be located at the interaction interface. In light of the final docking models, several important residues were identified as being responsible for Grp78–E2s binding. Table 4 lists all potential residues in contact, and Arg524 on E2s is highlighted as it ranked highly in both the hydrogen bond and  $\Delta$ SAS analysis.

**Table 4** Key residues in different interaction analysis

E2s <sup>a</sup>		Grp78	
H-Bond	SAS	H-Bond	SAS
Thr489A	Ser488A	Asp178	Ser406
Arg524A <sup>b</sup>	Arg524A <sup>b</sup>	Asn194	Gln409
Tyr561A	Pro525A	Val195	Gln530
Asn562A	Ser527A	Met196	Pro535
Thr586B	Gln530A	Asp410	Glu536
	Ala565A	Thr527	
	Gly589B	Asn528	

<sup>a</sup> A/B represent the two monomer chains of E2s

<sup>b</sup> Residues appearing in both analysis methods

Binding of Grp78 and E2s may interrupt the interaction between Grp78 and the J domain and interfere with allostereism between NBD and SBD

The Grp78 linker region has been proven to be involved in the interaction between Grp78 and other chaperone accessory proteins. The bovine Hsp70–J complex was discovered by Jiang et al. [17], who also found that the J domain activated the ATPase activity of Hsp70s by directing the NBD–SBD linker towards a hydrophobic patch on the NBD surface. Binding of the J domain to Hsp70 displaces the SBD from NBD, which may allow SBD more flexibility to capture diverse substrates. The binding of murine Grp78 and corresponding MTJ1 (homologous J chaperone) has also been reported and the ATPase stimulation noted [18]. Residues critical for the J chaperone–Hsp70 interaction have been identified as Lys170, Arg171, Asn174, Thr177, Ile179,

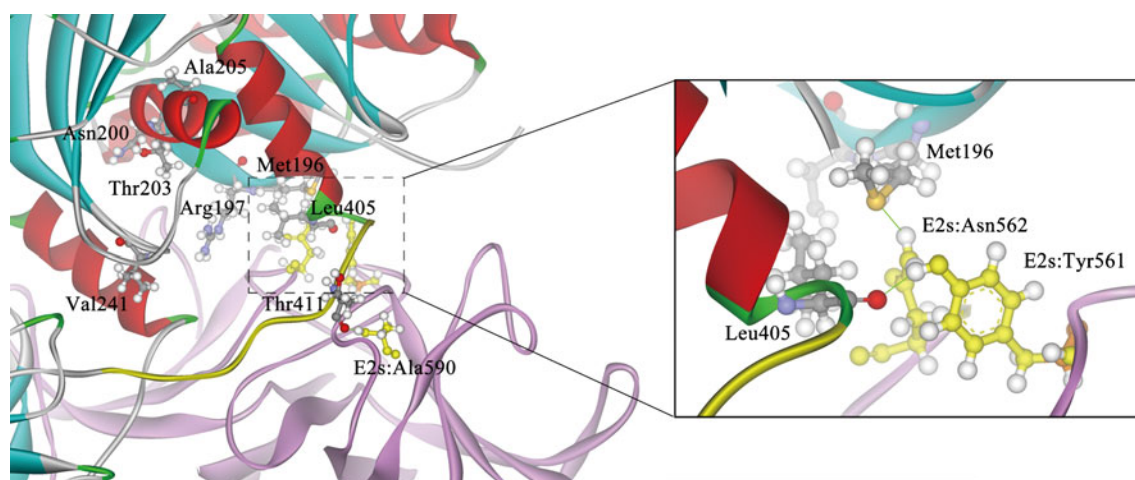


**Fig. 5** Spatial details of the cross sites of binding of Grp78 with E2s and the J domain. The complex is displayed as a solid ribbon diagram with Grp78 colored by secondary type. Pink E2s, yellow Grp78 linker. Key residues are rendered in ball-and-stick and colored by atom.

Different color schemes are adopted to differentiate the residues on Grp78 and E2s. The green line between the Grp78 and E2s residues represents hydrogen bonds

Ile216, Lys380 and Val388 [17], and the corresponding residues on Grp78 include Met196, Arg197, Asn200, Thr203, Ile205, Val241, Lys405 and Thr411 (Fig. 5). It can be clearly observed that most of these residues are involved in the Grp78:E2s interaction harboring at least three hydrogen bonds: (1) E2s:Asn562–Grp78:Met196, (2) E2s:Tyr561–Grp78:Leu405 and (3) E2s:Ala590–Grp78:Thr411. The first two hydrogen bonds are located on the inter-loop of 8 $\beta$ - and 9 $\beta$ -strands of the E2s monomer, targeting Grp78 NBD. The third is formed between the inter-loop of the 10 $\beta$ - and 11 $\beta$ - strands of the E2s monomer and the Grp78 linker region. The interface of Grp78:E2s and Grp78:J complex are overlapping, and Grp78 can bind E2s or J domain only alternatively in a competitive manner. Abundant intracellular E2s will inevitably block binding of the J domain to the linker region of Grp78, consequently decreasing the ATPase activity of NBD and eliminate the displacement of SBD from NBD, and finally abrogating the substrate peptide recognition of SBD. Compared with the previously published Hsp70–J structure, Grp78 binds with the loops linking  $\beta$ -strands of E2s, instead of the 2 $\alpha$ - and 3 $\alpha$ - helices of the J domain. The distinction in flexibility and contact profile of detailed secondary structures may elicit different binding affinities of these two kinds of ligands and implicate different biological functions. In general, the J chaperone acts as a presenter that binds Hsp70s with its J domain and presents the substrate to the SBD [39]. The simultaneous displacement of the NBD–SBD interaction could allow the SBD a greater range of motion so as to accept diverse substrates presented by different J co-chaperones. In this case, the interaction of Grp78 and E2s may diminish, or even prevent, subsequent substrate bindings. Another interesting finding is that the E2s:Asn562 residue involved in hydrogen bonding had been noted for its potential glycosylation site, and that a point mutation at Asn562 might prevent infection in macaques [40]. This result supports our docking model of Grp78:E2s, as Grp78 possibly participates in the endocytosis of HEV, and further investigation may help discover the underlying mechanism of HEV infection.

## Conclusions

Based on several homologous templates, a 3D structural model of protein Grp78 has been constructed by homology modeling and further optimized by MD simulation. The refined complex model of Grp78 and E2s elucidates putative structural details of interaction between Grp78 and E2s, and presents some key residues involved in the interaction. Comparing with the complex of Hsp70 and the J domain of J chaperone, we also concluded that the binding of E2s might block some normal functions of Grp78, including ATPase activity and substrate binding, and consequently

facilitate cell-entry of HEV and consequent infection. Furthermore, some residues in E2s (Arg524, Tyr561 and ASN562) were identified as being involved in interacting with Grp78, and should be subjected to site-directed mutation and functional validation in forthcoming investigations. In conclusion, the present study might provide some structural information giving further insights into the infection mechanism of HEV and the role of Grp78 in the host cell life cycle.

**Acknowledgments** The authors would like to acknowledge funding support from the National Natural Science Foundation (Grant no. 30925030, 30600106, 30870514, 30972826) and Project 863 (Grant no. 2006AA020905, 2006AA02A209), the great project on infectious diseases and new drug (Grant no. 2009ZX09102-230, 2009ZX10004-704, 2008ZX10404), People's Republic of China.

## References

- Jaiswal SP, Jain AK, Naik G, Soni N, Chitnis DS (2001) Viral hepatitis during pregnancy. *Int J Gynaecol Obstet* 72:103–108
- Xing L, Kato K, Li T, Takeda N, Miyamura T, Hammar L, Cheng RH (1999) Recombinant hepatitis E capsid protein self-assembles into a dual-domain T=1 particle presenting native virus epitopes. *Virology* 265:35–45
- Li S, Tang X, Seetharaman J, Yang C, Gu Y, Zhang J, Du H, Shih JWK, Hew CL, Sivaraman J, Xia N (2009) Dimerization of hepatitis E virus capsid protein E2s domain is essential for virus–host interaction. *PLoS Pathog* 5(8):e1000537. Epub 7 Aug 2009
- Wu XC, He SZ, Zheng ZZ, Sun YY, Zhang J, Xia NS (2006) Screening of protein interacting with hepatitis E virus nucleoprotein in HepG2 Cell. *Bing Du Xue Bao* 22:5
- Wu XC, Miao J, Zheng ZZ, He SZ, Sun YY, Tang M, Zhang J, Xia NS (2007) Grp78/Bip facilitates the attachment/entry of the hepatitis E virus capsid protein to host cells. *J Microb Infect* 2:5
- Chappell TG, Konforti BB, Schmid SL, Rothman JE (1987) The ATPase core of a clathrin uncoating protein. *J Biol Chem* 262:746–751
- Flaherty KM, DeLuca-Flaherty C, McKay DB (1990) Three-dimensional structure of the ATPase fragment of a 70 K heat-shock cognate protein. *Nature* 346:623–628
- Zhu X, Zhao X, Burkholder WF, Gragerov A, Ogata CM, Gottesman ME, Hendrickson WA (1996) Structural analysis of substrate binding by the molecular chaperone DnaK. *Science* 272:1606–1614
- Wang H, Kurochkin AV, Pang Y, Hu W, Flynn GC, Zuiderweg ER (1998) NMR solution structure of the 21 kDa chaperone protein DnaK substrate binding domain: a preview of chaperone–protein interaction. *Biochemistry* 37:7929–7940
- Morris JA, Dorner AJ, Edwards CA, Hendershot LM, Kaufman RJ (1997) Immunoglobulin binding protein (BiP) function is required to protect cells from endoplasmic reticulum stress but is not required for the secretion of selective proteins. *J Biol Chem* 272:4327–4334
- Peluso RW, Lamb RA, Choppin PW (1978) Infection with paramyxoviruses stimulates synthesis of cellular polypeptides that are also stimulated in cells transformed by Rous sarcoma virus or deprived of glucose. *Proc Natl Acad Sci USA* 75:6120–6124
- Bitko V, Barik S (2001) An endoplasmic reticulum-specific stress-activated caspase (caspase-12) is implicated in the apoptosis of A549 epithelial cells by respiratory syncytial virus. *J Cell Biochem* 80:441–454



13. Li XD, Lankinen H, Putkuri N, Vapalahti O, Vaheiri A (2005) Tula hantavirus triggers pro-apoptotic signals of ER stress in Vero E6 cells. *Virology* 333:180–189
14. Jordan R, Wang L, Graczyk TM, Block TM, Romano PR (2002) Replication of a cytopathic strain of bovine viral diarrhea virus activates PERK and induces endoplasmic reticulum stress-mediated apoptosis of MDBK cells. *J Virol* 76:9588–9599
15. Watowich SS, Morimoto RI, Lamb RA (1991) Flux of the paramyxovirus hemagglutinin-neuraminidase glycoprotein through the endoplasmic reticulum activates transcription of the GRP78-BiP gene. *J Virol* 65:3590–3597
16. Choukhi A, Ung S, Wychowski C, Dubuisson J (1998) Involvement of endoplasmic reticulum chaperones in the folding of hepatitis C virus glycoproteins. *J Virol* 72:3851–3858
17. Jiang J, Maes EG, Taylor AB, Wang L, Hinck AP, Lafer EM, Sousa R (2007) Structural basis of J cochaperone binding and regulation of Hsp70. *Mol Cell* 28:422–433
18. Chevalier M, Rhee H, Elguindi EC, Blond SY (2000) Interaction of murine BiP/GRP78 with the DnaJ homologue MTJ1. *J Biol Chem* 275:19620–19627
19. Chang YW, Sun YJ, Wang C, Hsiao CD (2008) Crystal structures of the 70-kDa heat shock proteins in domain disjoining conformation. *J Biol Chem* 283:15502–15511
20. Jiang J, Prasad K, Lafer EM, Sousa R (2005) Structural basis of interdomain communication in the Hsc70 chaperone. *Mol Cell* 20:513–524
21. Pellecchia M, Montgomery DL, Stevens SY, van der Kooi CW, Feng HP, Gierasch LM, Zuiderweg ER (2000) Structural insights into substrate binding by the molecular chaperone DnaK. *Nat Struct Biol* 7:298–303
22. Wilbanks SM, McKay DB (1995) How potassium affects the activity of the molecular chaperone Hsc70. II. Potassium binds specifically in the ATPase active site. *J Biol Chem* 270:2251–2257
23. Brooks BR, Brucoleri RE, Olafson DJ, States DJ, Swaminathan S, Karplus M (1983) CHARMM: a program for macromolecular energy, minimization, and dynamics calculations. *J Comput Chem* 4:187–217
24. Luthy R, Bowie JU, Eisenberg D (1992) Assessment of protein models with three-dimensional profiles. *Nature* 356:83–85
25. Chen R, Li L, Weng Z (2003) ZDOCK: an initial-stage protein-docking algorithm. *Proteins* 52:80–87
26. Chen R, Tong W, Mintseris J, Li L, Weng Z (2003) ZDOCK predictions for the CAPRI challenge. *Proteins* 52:68–73
27. Yan YQ, Li SW, Yang CY, Luo WX, Wang MQ, Chen YX, Luo HF, Wu T, Zhang J, Xia NS (2008) Prediction of a common neutralizing epitope of H5N1 avian influenza virus by in silico molecular docking. *Chin Sci Bull* 53:868–877
28. Morshauer RC, Hu W, Wang H, Pang Y, Flynn GC, Zuiderweg ER (1999) High-resolution solution structure of the 18 kDa substrate-binding domain of the mammalian chaperone protein Hsc70. *J Mol Biol* 289:1387–1403
29. Wisniewska M, Karlberg T, Lehtio L, Johansson I, Kotenyova T, Moche M, Schuler H (2010) Crystal structures of the ATPase domains of four human Hsp70 isoforms: HSPA1L/Hsp70-hom, HSPA2/Hsp70-2, HSPA6/Hsp70B', and HSPA5/BiP/GRP78. *PLoS ONE* 5:e8625
30. Bhattacharya A, Wunderlich Z, Monleon D, Tejero R, Montelione GT (2008) Assessing model accuracy using the homology modeling automatically software. *Proteins* 70:105–118
31. Li SW, Zhang J, He ZQ, Gu Y, Liu RS, Lin J, Chen YX, Ng MH, Xia NS (2005) Mutational analysis of essential interactions involved in the assembly of hepatitis E virus capsid. *J Biol Chem* 280:3400–3406
32. Zhang J, Gu Y, Ge SX, Li SW, He ZQ, Huang GY, Zhuang H, Ng MH, Xia NS (2005) Analysis of hepatitis E virus neutralization sites using monoclonal antibodies directed against a virus capsid protein. *Vaccine* 23:2881–2892
33. Guu TS, Liu Z, Ye Q, Mata DA, Li K, Yin C, Zhang J, Tao YJ (2009) Structure of the hepatitis E virus-like particle suggests mechanisms for virus assembly and receptor binding. *Proc Natl Acad Sci USA* 106:12992–12997
34. Yamashita T, Mori Y, Miyazaki N, Cheng RH, Yoshimura M, Unno H, Shima R, Moriishi K, Tsukihara T, Li TC, Takeda N, Miyamura T, Matsuura Y (2009) Biological and immunological characteristics of hepatitis E virus-like particles based on the crystal structure. *Proc Natl Acad Sci USA* 106:12986–12991
35. He S, Miao J, Zheng Z, Wu T, Xie M, Tang M, Zhang J, Ng MH, Xia N (2008) Putative receptor-binding sites of hepatitis E virus. *J Gen Virol* 89:245–249
36. Kim KS, Oh KS, Lee JY (2000) Catalytic role of enzymes: short strong H-bond-induced partial proton shuttles and charge redistributions. *Proc Natl Acad Sci USA* 97:6373–6378
37. Kim KS, Kim D, Lee JY, Tarakeshwar P, Oh KS (2002) Catalytic mechanism of enzymes: preorganization, short strong hydrogen bond, and charge buffering. *Biochemistry* 41:5300–5306
38. Zhou H, Singh NJ, Kim KS (2006) Homology modeling and molecular dynamics study of West Nile virus NS3 protease: a molecular basis for the catalytic activity increased by the NS2B cofactor. *Proteins* 65:692–701
39. Walsh P, Bursac D, Law YC, Cyr D, Lithgow T (2004) The J-protein family: modulating protein assembly, disassembly and translocation. *EMBO Rep* 5:567–571
40. Graff J, Zhou YH, Torian U, Nguyen H, St Claire M, Yu C, Purcell RH, Emerson SU (2008) Mutations within potential glycosylation sites in the capsid protein of hepatitis E virus prevent the formation of infectious virus particles. *J Virol* 82:1185–1194